Quenching by Oxygen of the Lowest Singlet and Triplet States of Pyrene and the Efficiency of the Formation of Singlet Oxygen in Liquid Solution under High Pressure

Masami Okamoto*,† and Fujio Tanaka‡

Faculty of Engineering and Design, Kyoto Institute of Technology, Matsugasaki, Sakyo-ku, Kyoto 606-8585, Japan, and College of Integrated Arts and Sciences, Osaka Prefecture University, Gakuencho, Sakai 599-8531, Japan

Received: October 2, 2001; In Final Form: December 20, 2001

Quenching by oxygen of the lowest singlet (S_1) and triplet (T_1) states of pyrene at pressures up to 400 MPa in liquid solution was investigated. The rate constant of the S_1 state, k_q^S, decreased significantly with increasing pressure, while that of the T_1 state, k_q^T, was nearly independent of pressure at the lower pressure region (<100 MPa) and decreased monotonically with further increase in pressure. The activation volume for k_q^S, $\Delta V_q^{S\ddagger}$, at 0.1 MPa fell in the range of 12−16 cm^3/mol, depending on the solvents examined, whereas that for k_q^T, $\Delta V_q^{T\ddagger}$, was nearly zero. It was found that both the activation volumes, $\Delta V_q^{S\ddagger}$ and $\Delta V_q^{T\ddagger}$, are significantly smaller than those determined from the pressure dependence of the solvent viscosity, η, $\Delta V_\eta^{\ddagger}$ (22−25 cm^3/mol). For the quenching of the S_1 state, the large difference between $\Delta V_q^{S\ddagger}$ and $\Delta V_\eta^{\ddagger}$ was interpreted in terms of the competition of the quenching with diffusion, and k_q^S was separated into the contributions of the rate constants for diffusion, k_{diff}, and for the bimolecular quenching in the solvent cage, $k^{S,bim}$. For the quenching of the T_1 state, it was found that k_q^T/k_{diff} increases over 1/9 and approaches 4/9 with increasing pressure. The oxygen concentration dependence on the quantum yield for the formation of singlet oxygen, Φ_Δ, in methylcylohexane (MCH) was measured at pressures up to 400 MPa in order to separate Φ_Δ into the contributions of the S_1 and T_1 states. From the results, together with those of the pressure dependence of the quantum yield of T_1 state, the branching ratio for the formation of singlet oxygen in the T_1 state, f_Δ^T, was found to decrease with increasing pressure. The oxygen quenching of the T_1 state from these results was discussed by using the mechanism that involves the encounter complex pairs with singlet, triplet, and quintet spin multiplicities.

Introduction

The quenching by oxygen of the lowest electronically excited singlet state (S_1) of aromatic molecules in solution has been extensively investigated,[1−3] and it is often believed to be diffusion-controlled. In fact, the quenching rate constant of the S_1 state, k_q^S, in nonviscous solvents is on the order of 10^{10} M^{-1} s^{-1}, which is close to the rate constant for diffusion calculated by the Debye equation in a continuum medium with viscosity, η.

$$k_{diff} = \frac{8RT}{\alpha\eta} \tag{1}$$

where α is 2000 and 3000 for the slip and stick boundary limits, respectively.[1−5] However, the expression of eq 1 has often failed in experiments in which η was changed by changing temperature and solvent at atmospheric pressure.[4−5] This is attributed to lack of the $1/\eta$ dependence of the diffusion coefficients of fluorophore and/or quencher,[6,7] which may be caused by the neglect of the difference in size of the solute and solvent molecules, and also by the deviation from the continuum model that arises as a result of short-range interactions between the solute and solvent molecules such as translational and rotational coupling.

An empirical equation developed by Spernol and Wirtzs,[8,9] for which α in eq 1 is replaced by α^{SW}, that depends on the properties of the solvent and solute molecules has been applied successfully to diffusion-controlled radical self-termination reactions,[10] exothermic triplet excitation transfer,[2,11,12] and various types of reactions in supercritical carbon dioxide as well as in liquid solution by changing temperature and pressure.[13−17]

High-pressure studies have also clearly revealed that the fluorescence quenching by oxygen of the S_1 state of a number of meso-substituted anthracene derivatives is diffusion-controlled in nature from the pressure-induced solvent viscosity dependence at a constant temperature.[18,19] Very recently, we have examined the fluorescence quenching of some aromatic molecules by heavy atoms and oxygen in liquid solution at high pressure, and found that the fluorescence quenching by oxygen and carbon tetrabromide is not fully but nearly diffusion-controlled.[14−16] From the analysis of the pressure-induced solvent viscosity dependence of the observed quenching rate constant, the contribution of diffusion to the quenching was separated into the bimolecular rate constant for diffusion, k_{diff}, and that for the quenching in the solvent cage. The separation was successfully applied to the fluorescence quenching of pyrene by polybromoethanes and carbon tetrabromide,[14] and benzo[*a*]-pyrene[15] and 9,10-dimethylanthracene[16] by oxygen and carbon tetrabromide. The value of k_{diff} estimated by the analysis was found to be in good agreement with those determined by eq 1 using α^{SW} and η.

The quenching by oxygen of the lowest triplet state, T_1, is not efficient as compared to that of the S_1 state for most aromatic compounds, and the quenching rate constant, k_q^T, is on the order

† Kyoto Institute of Technology.
‡ Osaka Prefecture University.

10.1021/jp013675c CCC: $22.00
Published on Web 03/19/2002

SCHEME 1

$$^3M^* + O_2(^3\Sigma_g^-) \underset{k_{-diff}}{\overset{5/9k_{diff}}{\rightleftharpoons}} {}^5(MO_2)^*$$

$$^3M^* + O_2(^3\Sigma_g^-) \underset{k_{-diff}}{\overset{3/9k_{diff}}{\rightleftharpoons}} {}^3(MO_2)^* \xrightarrow{k_{ic}{}^T} M + O_2(^3\Sigma_g^-)$$

$$^3M^* + O_2(^3\Sigma_g^-) \underset{k_{-diff}}{\overset{1/9k_{diff}}{\rightleftharpoons}} {}^1(MO_2)^* \xrightarrow{k_{et}{}^T} M + O_2(^1\Delta_g)$$

of 10^9 M^{-1} s^{-1} for typical aromatic hydrocarbons.[2] The less efficient quenching of the T_1 state has been explained by the mechanism shown in Scheme 1, in which encounter complex pairs $^i(MO_2)^*$ (i = 1, 3, or 5) with three different spin multiplicities are involved.[20]

In Scheme 1, $^i(MO_2)^*$ (i = 1, 3 or 5) is formed with $i/9$ of the diffusion-controlled rate constant, k_{diff}, by the requirement of spin statistics. Thus, the low quenching ability of the T_1 state has been explained by the participation of $^i(MO_2)^*$(i = 1 and 3) that leads to the quenching. The yield of singlet oxygen ($O_2(^1\Delta_g)$), $f_\Delta{}^T$, by the quenching of the T_1 state, $^3M^*$, is close to unity for most anthracene derivatives,[21,22] indicating that k_{ic} is closed in Scheme 1, whereas it is less than unity for some ketones[23,24] and nearly unity for some aromatic hydrocarbons[25−27] including pyrene.[28−30] The intersystem crossing between the encounter complex pairs has been proposed to be involved in the quenching for systems with internal heavy atom effects[31] and charge transfer interactions.[32,33]

According to Scheme 1, when the quenching of the T_1 state occurs with the fully diffusion-controlled rate, $k_q{}^T = k_{diff}/9$ for $f_\Delta{}^T = 1$ and $k_q{}^T = 4k_{diff}/9$ for $f_\Delta{}^T = 1/4$. In a previous paper,[34] we measured the quenching rate constant, $k_q{}^T$, by oxygen of the T_1 state of 9-acetylanthracene that is approximately nonfluorescent (triplet quantum yield for T_1 state, Φ_T, is nearly unity)[35] and that of S_1 state of 9,10-dimethylanthracene, $k_q{}^S$, in liquid solution at high pressure. It was found that the ratio $k_q{}^T/k_q{}^S$, where $k_q{}^S$ is assumed to be nearly equal to k_{diff}, increases with increasing pressure in the solvents examined. From the results, together with findings that both the quantum yields of the T_1 state of 9-acetylanthracene and of the formation of singlet oxygen sensitized by it are unity and independent of pressure, it was concluded that the intersystem crossing between the encounter complex pairs involved in Scheme 1 is enhanced by pressure.

The quenching of the S_1 state by oxygen may involve an encounter complex pair, $^1(MO_2)^*$, with singlet spin multiplicity, which leads to the formation of $^1O_2$ with an efficiency $f_\Delta{}^S$.[2,21,22,28−30,36] It has been found that the contribution of $f_\Delta{}^S$ to the total quantum yield of singlet oxygen by the oxygen quenching of the S_1 and T_1 states at infinite oxygen concentration, Φ_Δ, is not significant for pyrene; $f_\Delta{}^S = 0.15$ ($\Phi_\Delta = 1.2$)[28] and 0.13 (0.78)[29] in cyclohexane and $f_\Delta{}^S = 0.30$ (ca. 1.1) in acetonitrile.[30] However, for 9,10-dicyanoanthracene at infinite oxygen concentration Φ_Δ was reported to be ca. 2[21,28,37] with $f_\Delta{}^S = 1$. The evidence indicates that the mechanism of the oxygen quenching, which may involve not only the diffusion processes in liquid but also depend on the nature of the electronic state of the sensitizer examined, is still a problem to resolve.

In the present work, the quantum yield of singlet oxygen, Φ_Δ, as well as the quenching rate constants by oxygen of the T_1 and S_1 states of pyrene, $k_q{}^T$ and $k_q{}^S$, respectively, were measured as a function of pressure in nonpolar solvents at pressures up to 400 MPa in order to obtain further insight into the oxygen quenching of the S_1 and T_1 states. From the results, the quenching mechanism is discussed by focusing on (i) estimation of k_{diff} from $k_q{}^S$, (ii) the pressure dependence of $k_q{}^T/k_{diff}$, and (iii) the pressure dependence of $f_\Delta{}^T$ and $f_\Delta{}^S$.

Experimental Section

Pyrene (PY) (Wako Pure Chemicals Ltd.) was chromatographed twice on silica gel, developed and eluted with *n*-pentane, and recrystallized twice from ethanol. Solvents of *n*-pentane (Merck), *n*-hexane (Merck), and methylcyclohexane (MCH, Dojin Pure Chemicals Co.) of spectroscopic grade were used as received.

Transient absorption measurements at high pressure were performed by using an 8-ns pulse from a nitrogen laser (337.1 nm) for excitation and a xenon analyzing flash lamp positioned at right angles to the direction of the excitation pulse. The analyzing light intensities were monitored by a Hamamatsu R928 photomultiplier through a Ritsu MC-25N monochromator, and the signal was digitized by using a Hewlett-Packard 54510A digitizing oscilloscope. Fluorescence decay curve measurements at high pressure were performed by using a 0.3-ns pulse from a PRA LN103 nitrogen laser for excitation. The fluorescence intensities were measured by a Hamamatsu R1635-02 photomultiplier through a Ritsu MC-25NP monochromator, and the resulting signal was digitized by using a LeCroy 9362 digitizing oscilloscope. All data were analyzed by using a NEC 9801 microcomputer, which was interfaced to the digitizers. The details about the associated high-pressure techniques have been described elsewhere.[38,39]

The concentration of PY for the triplet lifetime measurements was adjusted to be ca. 0.8 in absorbance (1 cm cell) at 337.1 nm, and that for the fluorescence lifetime measurements was less than 0.1 at maximum absorption wavelength to minimize the reabsorption effects. In the measurements of T−T′ absorption spectra as a function of pressure, the higher concentration of PY (ca. 1.6) was chosen in order to minimize the concentration dependence on the number of absorbed photons. In these absorbance ranges, the concentration of PY corresponds to ca. 2×10^{-6} to 4×10^{-5} M at 0.1 MPa where the formation of the excimer is insignificant, especially at high pressure since the formation of the excimer is significantly retarded by increasing pressure.[40] The deoxygenation of the sample solution was carried out by bubbling nitrogen gas under nitrogen atmosphere at room temperature for *n*-hexane and MCH and at 0 °C for *n*-pentane. The concentrations of dissolved oxygen in those air-saturated solvents were determined from the solubility data of oxygen.[41,42] The increase in the concentration of oxygen by applying high pressure was corrected by using the compressibility of solvent.[43−47]

The phosphorescence decay curves of singlet oxygen at 1270 nm were measured as a function of pressure by a method similar to that described previously.[34,48,49] The element used in the near-IR detection system was replaced by an InGaAs sensor (1 mm ϕ, Hamamatsu G5832-01) which was biased reversely at 5 V since the time response is much better (the total rise time was about 0.4 μs).

The absorption spectra as a function of pressure were recorded on a Shimazu UV 260 equipped with the high-pressure optical cell. The spectra of the sample solution and the solvent were taken separately, and the corrected spectra were obtained by subtracting the latter from the former spectra.

Temperature was controlled at 25 ± 0.2 °C for the measurements of the lifetimes of the S_1 and T_1 states, and for those of the quantum yields of singlet oxygen and the T_1 state. Pressure

TABLE 1: Oxygen-Quenching Rate Constants for the S_1, k_q^S, and T_1, k_q^T, States of Pyrene in MCH at 25 °C[a]

P/MPa	η/cP	τ_f^0/ns	k_q^S [b]/10^{10} M^{-1} s^{-1}	τ_T/ns	$k_q^T/10^{10}$ M^{-1} s^{-1}
0.1	0.674	404	2.72 ± 0.01	161	0.249
50	1.143	393	2.01 ± 0.02	155	0.247
100	1.739	390	1.47 ± 0.01	164	0.227
150	2.542	388	1.12 ± 0.01	170	0.213
200	3.752	384	0.86 ± 0.01	181	0.197
250	5.146	380	0.68 ± 0.01	189	0.185
300	7.211	376	0.53 ± 0.01	209	0.165
350	10.02	374	0.42 ± 0.01	227	0.150
400	12.81	364	0.33 ± 0.01	267	0.126

[a] Errors of lifetimes and the quenching rate constant, k_q^T, were estimated to be about ± 3%. [b] Error was estimated from the standard deviation of the plot of $1/\tau_f$ against the oxygen concentration (see the text).

TABLE 2: Oxygen-Quenching Rate Constants for the S_1, k_q^S, and T_1, k_q^T, States of Pyrene in *n*-Pentane at 25 °C[a]

P/MPa	η/cP	τ_f^0/ns	$k_q^S/10^{10}$ M^{-1} s^{-1}	τ_T/ns	$k_q^T/10^{10}$ M^{-1} s^{-1}
0.1	0.229	363	3.46	244	0.177
50	0.350	359	2.67	213	0.188
100	0.484	359	2.16	203	0.189
150	0.629	359	1.80	200	0.185
200	0.786	357	1.51	202	0.178
250	1.002	351	1.29	205	0.172
300	1.202	354	1.13	208	0.166
350	1.443	353	1.00	217	0.157
400	1.726	348	0.88	224	0.150

[a] Errors of lifetimes and the quenching rate constants were estimated to be about ±3%.

TABLE 3: Oxygen-Quenching Rate Constants for the S_1, k_q^S, and T_1, k_q^T, States of Pyrene in *n*-Hexane at 25 °C[a]

P/MPa	η/cP	τ_f^0/ns	$k_q^S/10^{10}$ M^{-1} s^{-1}	τ_T/ns	$k_q^T/10^{10}$ M^{-1} s^{-1}
0.1	0.294	396	3.89	158	0.197
50	0.472	378	2.99	143	0.205
100	0.650	380	2.37	142	0.202
150	0.849	382	1.92	141	0.196
200	1.063	381	1.58	144	0.188
250	1.310	378	1.32	149	0.176
300	1.610	379	1.13	153	0.168
350	1.948	376	0.95	162	0.156
400	2.368	374	0.83	170	0.147

[a] Errors of lifetimes and the quenching rate constants were estimated to be about ±3%.

was measured by a calibrated manganin wire or a Minebea STD-5000K strain gauge.

Results

Rate Constants, k_q^S, for the Fluorescence Quenching. Fluorescence decay curves were analyzed satisfactorily by a single-exponential function under all the conditions examined. The fluorescence lifetimes in the absence of oxygen, τ_f^0, are listed in Tables 1−3 for MCH, *n*-pentane and *n*-hexane, respectively, together with the data of solvent viscosity, η.[43−47] The values of τ_f^0 are in good agreement with those in MCH and *n*-hexane reported previously.[40] The quenching rate constant for the S_1 state of PY, k_q^S, was determined by eq 2 since the concentration of dissolved oxygen is obtained from the solubility data.[41,42]

$$1/\tau_f - 1/\tau_f^0 = k_q^S[O_2] \quad (2)$$

where τ_f represents the fluorescence lifetime in the presence of oxygen. In MCH, the lifetime was measured for the sample containing three different concentrations of oxygen; the sample

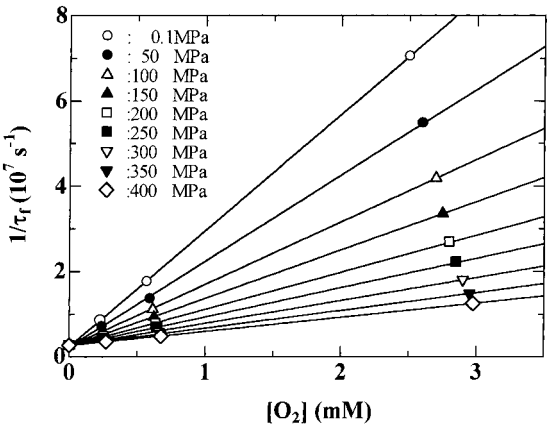

Figure 1. Plots of $1/\tau_f$ against concentration of oxygen, [O_2], in MCH.

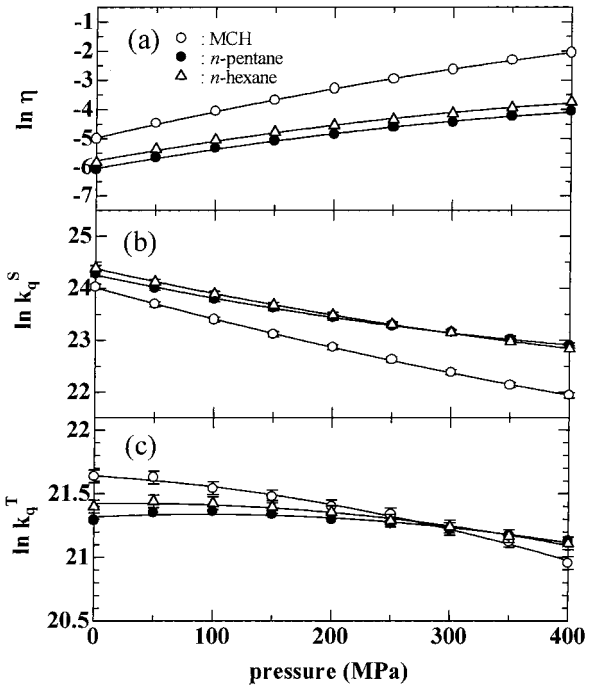

Figure 2. Pressure dependence of solvent viscosity, η (a), k_q^S (b), and k_q^T (c) in three solvents. The solid lines were drawn by assuming that $\ln \eta = A + BP + CP^2$ and $\ln k_q^i$ (i = S or T) $= A' + B'P + C'P^2$.

except for the air-saturated solution was prepared by bubbling the O_2/N_2 gas mixture with 1.903% and 4.76% oxygen. Figure 1 shows the plot of $1/\tau_f$ against [O_2]. The value of k_q^S was determined from the least-squares slope. The value of k_q^S thus determined was in very good agreement with those obtained by using the lifetimes in the aerated and deaerated solutions. In *n*-pentane and *n*-hexane, k_q^S was determined from the lifetimes in the aerated and deaerated solutions according to eq 2. The results obtained are listed in Tables 1−3.

As seen in Tables 1−3, k_q^S decreases significantly with increasing pressure in solvents studied in this work. The pressure dependence of k_q^S is shown in Figure 2, together with that of the solvent viscosity. The apparent activation volumes for k_q^S, $\Delta V_q^{S\ddagger}$, at 0.1 MPa, evaluated by eq 3 (i = S) are listed in Table 4, together with those for solvent viscosity, $\Delta V_\eta^{\ddagger}$, determined from Figure 2a.

$$RT(\partial \ln k_q^i/\partial P)_T = -\Delta V_q^{i\ddagger} \quad (3)$$

As seen in Table 4, the values of $\Delta V_q^{S\ddagger}$ are of the magnitude of 12−16 cm^3/mol, which lies in the range of positive activation

TABLE 4: Values of the Apparent Activation Volume (cm^3/mol) for the Solvent Viscosity, $\Delta V_\eta^{\ddagger}$, and k_q^i (i = S or T), $\Delta V_q{}^{i\ddagger}$, at 0.1 MPa and 25 °C, and Those of β_i (i = S) at 25 °C in Three Solvents

	$\Delta V_\eta^{\ddagger a}$	$\Delta V_q{}^{S\ddagger}$	$\Delta V_q{}^{T\ddagger}$	β_i (i = S)
n-pentane	22	11.9 ± 0.3	−1.1 ± 0.4	0.69 ± 0.01
n-hexane	24	12.6 ± 0.2	−0.3 ± 0.4	0.77 ± 0.02
MCH	25	15.6 ± 0.4	1.4 ± 0.5	0.71 ± 0.01

[a] $\Delta V_\eta^{\ddagger}$ was determined from the pressure dependence of the solvent viscosity, η, according to $(\partial \ln \eta/\partial P)_T = \Delta V_\eta^{\ddagger}/RT$.

volumes found for the nearly diffusion-controlled fluorescence quenching by oxygen of anthracene derivatives that have one or two electron-donating substituents.[19] The large difference between $\Delta V_q{}^{S\ddagger}$ and $\Delta V_\eta^{\ddagger}$ (see Table 4) may indicate that the fluorescence quenching of PY is not fully but nearly diffusion-controlled, as concluded previously for other quenching systems.[15,16] Another test for the nearly diffusion-controlled reaction is the fractional power dependence of η on $k_q{}^i$ (i = S), which is given by

$$k_q{}^i = A\eta^{-\beta_i} \tag{4}$$

where A is independent of pressure and $0 < \beta_i \leq 1$.[19] In fact, the plots of ln $k_q{}^S$ against ln η are almost linear in the solvents examined, and the values of β_i (i = S) determined by the least-squares plots are listed in Table 4. The β_i value (i = S) is less than unity in the solvents examined, also indicating that the fluorescence quenching by oxygen is not fully but nearly diffusion-controlled.[15,16]

Quenching Rate Constants, $k_q{}^T$, for the T_1 State. The decay curves of the T−T′ absorption were described satisfactorily by a single-exponential function under all the conditions examined. The quenching rate constant for the T_1 state, $k_q{}^T$, was determined by

$$1/\tau_T - 1/\tau_T{}^0 = k_q{}^T[O_2] \tag{5}$$

where τ_T and $\tau_T{}^0$ are the triplet-state lifetimes of PY in the aerated and deaerated solutions, respectively. In the determination of $k_q{}^T$, the term $1/\tau_T{}^0$ was neglected since $\tau_T{}^0$ is significantly longer than τ_T. The values of of $k_q{}^T$ in MCH, *n*-pentane, and *n*-hexane are listed in Tables 1, 2, and 3, respectively, together with those of τ_T.

As seen in Tables 1−3, the pressure dependence of $k_q{}^T$ is significantly smaller compared to that of $k_q{}^S$ in the solvents examined. It is also found that $k_q{}^T/k_q{}^S$ at 0.1 MPa is 0.092, 0.052, and 0.051 in MCH, *n*-pentane, and *n*-hexane, respectively; they are smaller than 1/9, indicating that the step of $k_q{}^T$ is not fully diffusion-controlled. The pressure dependence of $k_q{}^T$ is shown in Figure 2c, and the apparent activation volumes for $k_q{}^T$, $\Delta V_q{}^{T\ddagger}$, evaluated by eq 3 (i = T) at 0.1 MPa are listed in Table 4, in which the magnitude of $\Delta V_q{}^{T\ddagger}$ is nearly equal to that for anthracene derivatives with electron-donating substituents.[19] The plots of ln $k_q{}^T$ against ln η, which were nearly linear for the fluorescence quenching as mentioned in the previous section, showed significant downward curvatures in the solvents examined. For example, the value of β_i (i = T) (see eq 4) increased monotonically from −0.12 at 0.1 MPa to 0.25 at 400 MPa in *n*-pentane. These observations are common to the quenching by oxygen of the T_1 states of the anthracene derivatives,[18,19] suggesting that the encounter pairs with three spin multiplicities are involved in the quenching processes (see Scheme 1).

Pressure Dependence of Triplet Quantum Yield in MCH. The pressure dependence of the T−T′ absorption spectra of PY in MCH is shown in Figure 3. As seen in Figure 3, the spectra show a gradual red shift, but the maximum intensity does not change significantly with increasing pressure in the absence of oxygen. Similar observations were found in the presence of oxygen (Figure 3b), although the maximum intensity is about 2.5 times larger compared to that in the absence of oxygen. This suggests that the quantum yield for the formation of the T_1 state is approximately independent of pressure irrespective of the presence and absence of oxygen provided that the pressure dependence of the molar extinction coefficient, ϵ, is not significant. Unfortunately, there are no available data on the pressure dependence of ϵ for the T_1 state to our knowledge. Figure 4 shows the absorption spectra of PY in MCH at pressures up to 400 MPa. In Figure 4, we can see the red shift and slight increase in bandwidth with increasing pressure; they are the normally observed pressure dependence for the absorption spectra. However, the values of ϵ at the maximum wavelengths of 319.10 and 334.85 nm (0.1 MPa) are nearly independent of pressure when the concentration is corrected by the solvent density: the ratio of ϵ at P MPa to that at 0.1 MPa, $\epsilon(P)/\epsilon(0.1)$, is 1.02, 1.03, 1.03, and 1.03 at 100, 200, 300, and 400 MPa, respectively, for the band at 334.85 nm (0.1 MPa). The evidence may support that ϵ of the T_1 state is reasonably assumed to be independent of pressure.

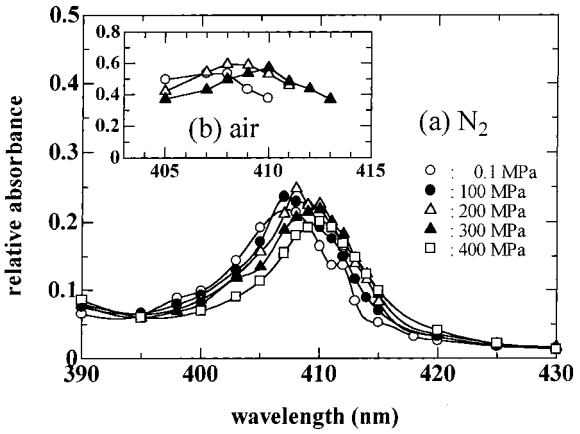

Figure 3. Transient absorption spectra of pyrene extrapolated at time 0 after the laser pulse excitation in deoxygenated (a) and air-saturated (b) MCH.

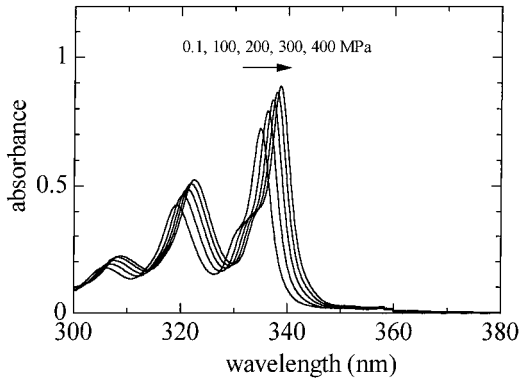

Figure 4. Pressure dependence of absorption spectra of pyrene in MCH.

Pressure Dependence of the Yield of Singlet Oxygen in Air-Saturated Solutions. The values of the lifetime of singlet oxygen, τ_Δ, determined by the phosphorescence decay measurements in the solvents examined decreased significantly with increasing pressure; for example, τ_Δ decreased from 24.8 to 11.3

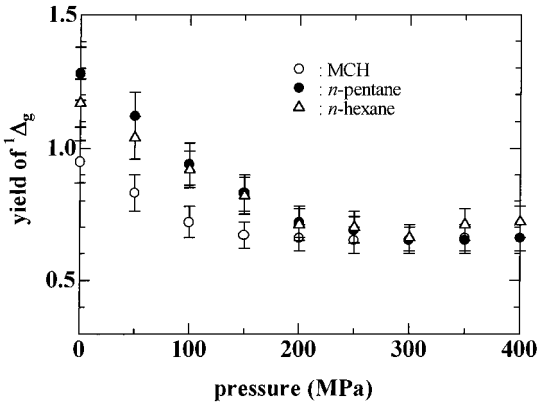

Figure 5. Pressure dependence of yield for formation of singlet oxygen ($^1\Delta_g$) in three air-saturated solvents.

μs in MCH on going from 0.1 to 400 MPa. Such a pressure dependence of the decrease in the lifetime, which occurs via the collision with the solvent molecules, may be explained in the framework of the works reported by us[48−50] and others,[51] and hence, no further discussion is made here.

The phosphorescence intensity extrapolated to time 0 was examined for the air-saturated samples with absorbances (0.1 MPa; 1 cm path length) of 0.20, 0.30, and 0.43 at 337.1 nm and was found to increase approximately linearly with increasing absorbance at each pressure. The absorbance of PY at 337.1 nm obtained by measurements of the absorption spectra increased by 1.8 times with a maximum (2.3 times) at 200 MPa when pressure increased from 0.1 to 400 MPa in MCH. In previous work,[34] the quantum yield of singlet oxygen sensitized by 9-acetylanthracene (ACA) in *n*-pentane, *n*-hexane, and MCH was measured and was found to be unity at pressures up to 400 MPa. The quantum yield for PY, Φ_Δ, in three air-saturated solvents was evaluated at pressures up to 400 MPa by comparing the intensity extrapolated to time 0 for PY with that for ACA as a standard in the same solvent at each pressure, together with the values of absorbances at 337.1 nm of PY and ACA. The pressure dependence of Φ_Δ of PY in those air-saturated solvents is shown in Figure 5. As seen in Figure 5, Φ_Δ, which involves contributions from both the S_1 and T_1 states, decreases monotonically with increasing pressure.

Singlet Oxygen Yield for the Oxygen Quenching of the S_1 and T_1 States in MCH. In general, singlet oxygen formation by the oxygen quenching of both the $S_1$and T_1 states may be expressed in Scheme 2,

SCHEME 2

$$^1M^* + {}^3O_2(^3\Sigma_g^-) \xrightarrow{k_q^{S,\Sigma}} {}^3M^* + {}^3O_2(^3\Sigma_g^-)$$

$$^1M^* + {}^3O_2(^3\Sigma_g^-) \xrightarrow{k_q^{S,\Delta}} {}^3M^* + {}^3O_2(^1\Delta_g)$$

$$^3M^* + {}^3O_2(^3\Sigma_g^-) \xrightarrow{k_q^{T,\Sigma}} M + {}^3O_2(^3\Sigma_g^-)$$

$$^3M^* + {}^3O_2(^3\Sigma_g^-) \xrightarrow{k_q^{T,\Delta}} M + {}^3O_2(^1\Delta_g)$$

where $k_q^S = k_q^{S,\Sigma} + k_q^{S,\Delta}$ and $k_q^T = k_q^{T,\Sigma} + k_q^{T,\Delta}$. The quantum yield of singlet oxygen via the S_1 state, Φ_Δ^S, is expressed by eq 6 as follows:

$$\Phi_\Delta^S = f_\Delta^S \left(\frac{\tau_f^0 k_q^S[O_2]}{1 + \tau_f^0 k_q^S[O_2]} \right) \tag{6}$$

In eq 6, the branching ratio in the S_1 state, f_Δ^S, is given by

$$f_\Delta^S = \frac{k_q^{S,\Delta}}{k_q^{S,\Sigma} + k_q^{S,\Delta}} \tag{7}$$

Similarly, the quantum yield of singlet oxygen via the T_1 state, Φ_Δ^T, is given by eq 8 as follows:

$$\Phi_\Delta^T = f_\Delta^T \Phi_T^{ox} = f_\Delta^T \left(\frac{\Phi_T + \tau_f^0 k_q^S[O_2]}{1 + \tau_f^0 k_q^S[O_2]} \right) \tag{8}$$

where Φ_T^{ox} and Φ_T are the quantum yields of T_1 state in the presence and absence of oxygen, respectively. The branching ratio in the T_1 state, f_Δ^T, is given by

$$f_\Delta^T = \frac{k_q^{T,\Delta}}{k_q^{T,\Sigma} + k_q^{T,\Delta}} \tag{9}$$

Therefore, the overall quantum yield of singlet oxygen, Φ_Δ, is expressed by

$$\Phi_\Delta = \Phi_\Delta^S + \Phi_\Delta^T = \Phi_\Delta^S + f_\Delta^T \Phi_T^{ox} \tag{10}$$

To determine f_Δ^S and f_Δ^T, Φ_Δ was measured as a function of the concentration of oxygen at pressures up to 400 MPa, where the sample was prepared by bubbling the oxygen−nitrogen gas mixture containing 1.903% and 4.76% oxygen other than the aerated MCH solution. The concentration dependence of oxygen on Φ_Δ is described by eq 11 from eqs 6 and 8.

$$(1 + \tau_f^0 k_q^S[O_2])\Phi_\Delta = (f_\Delta^S + f_\Delta^T)\tau_f^0 k_q^S[O_2] + f_\Delta^T \Phi_T \tag{11}$$

Figure 6a shows the plot of $(1 + \tau_f^0 k_q^S[O_2])\Phi_\Delta$ against $\tau_f^0 k_q^S[O_2]$ in MCH. From the least-squares slope and intercept of the plot shown in Figure 6a, the values of $f_\Delta^S + f_\Delta^T$ and $f_\Delta^T \Phi_T$, respectively, were determined, and the pressure dependence of $f_\Delta^S + f_\Delta^T$ and $f_\Delta^T \Phi_T$ is shown in Figure 6b. It can be

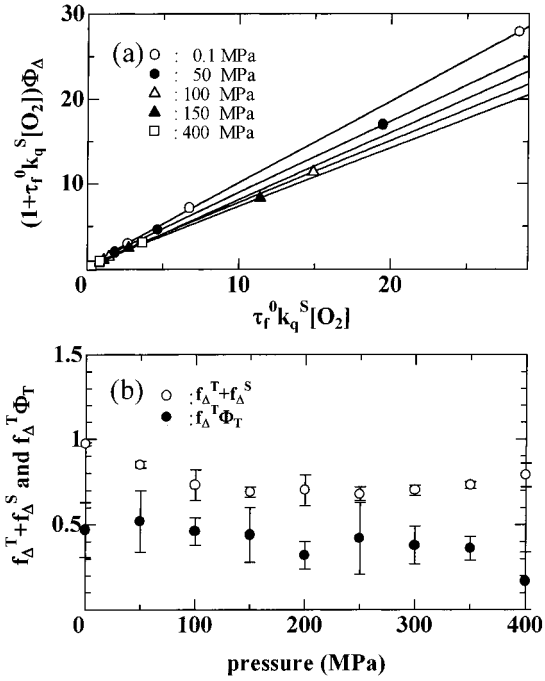

Figure 6. Plots of $(1 + \tau_f^0 k_q^S[O_2])\Phi_\Delta$ against $\tau_f^0 k_q^S[O_2]$ at five pressures (a) and pressure dependence of $f_\Delta^T + f_\Delta^S$ and $f_\Delta^T \Phi_T$ (b) in MCH.

seen in Figure 6b that both $f_\Delta^S + f_\Delta^T$ and $f_\Delta^T\Phi_T$ decrease with increasing pressure although the latter has large errors. The pressure dependence of $f_\Delta^T\Phi_T$ suggests that f_Δ^T tends to decrease with increasing pressure since Φ_T is approximately independent of pressure as mentioned above; by assuming 0.5 in cyclohexane[28] as Φ_T, f_Δ^T decreases monotonically from 0.9 ± 0.4 to 0.3 ± 0.3 when pressure increases from 0.1 to 400 MPa. Unfortunately, the values of f_Δ^S cannot be determined because of large error.

Discussion

In the present section, we first evaluate the rate constants for diffusion, k_{diff}, and for the bimolecular quenching of the S_1 state in the solvent cage, $k^{S,bim}$, from the pressure-induced solvent viscosity dependence of k_q^S. Then, from the results of the pressure dependence of k_{diff} and k_q^T, together with those of the yield of singlet oxygen, the mechanism of the quenching of the T_1 state by oxygen in liquid solution is discussed.

Separation of k_q^S into k_{diff} and $k^{S,bim}$. In previous publications,[14−17] we have shown that the observed fluorescence quenching rate constant, k_q^S, with a nearly diffusion-controlled rate in liquid solution can be separated into the bimolecular rate constant for diffusion, k_{diff}, and that for the quenching in the solvent cage, $k^{S,bim}$. In general, the fluorescence quenching by oxygen in liquid solution may occur via an encounter complex with singlet spin multiplicity, $^1(MO_2)^*$, Scheme 3.[52]

SCHEME 3

$$^1M^* + O_2 \underset{k_{-diff}}{\overset{k_{diff}}{\rightleftharpoons}} {}^1(MO_2)^* \xrightarrow{k_{ic}^S} {}^3M^* + O_2(^3\Sigma_g^-)$$

$$^1M^* + O_2 \underset{k_{-diff}}{\overset{k_{diff}}{\rightleftharpoons}} {}^1(MO_2)^* \xrightarrow{k_{et}^S} {}^3M^* + O_2(^1\Delta_g)$$

On the basis of this scheme, k_q^S is expressed by

$$k_q^S = \frac{k_{diff}k^S}{k_{-diff} + k^S} \tag{12}$$

where $k^S = k_{ic}^S + k_{et}^S$. In eq 12, $k_q^S = k_{diff}$ if $k^S \gg k_{-diff}$ and $k_q^S = k_{diff}k^S/k_{-diff}$ if $k_{-diff} \gg k^S$; the quenching occurs upon every encounter for the former case, whereas the quenching efficiency is less than unity for the latter case. When k_{diff} is assumed to be expressed by eq 1 (α in eq 1 is replaced by α^{ex}), we have[13,14]

$$\frac{1}{k_q^S} = \frac{1}{k^S}\left(\frac{k_{-diff}}{k_{diff}}\right) + \frac{\alpha^{ex}}{8RT}\eta \tag{13}$$

In eq 13, the pressure dependence of k_{diff}/k_{-diff} is given by that of the radial distribution function, $g(r_{M^*Q})$, at the closest approach distance (the encounter distance), r_{M^*Q} ($=r_{M^*} + r_Q$; the sum of the radius of $^1M^*$, r_{M^*}, and the quencher, Q, r_Q), with hard spheres. Thus, the following equation may be derived:

$$\frac{\gamma}{k_q^S} = \frac{1}{k^S}\left(\frac{k_{-diff}}{k_{diff}}\right)_0 + \frac{\alpha^{ex}}{8RT}\eta\gamma \tag{14}$$

where γ is the ratio of $g(r_{M^*Q})$ at P MPa to that at 0.1 MPa, $g(r_{M^*Q})/g(r_{M^*Q})_0$, and $(k_{-diff}/k_{diff})_0$ is k_{-diff}/k_{diff} at 0.1 MPa. According to eq 14, the plot of γ/k_q^S against $\gamma\eta$ should be linear when k^S is independent of pressure.

The plot of γ/k_q^S against $\gamma\eta$ is shown in Figure 7.[53] All the plots shown in Figure 7 are approximately linear with positive intercepts, indicating that the quenching competes with diffusion, and also indicating that k^S is independent of pressure. These observations are consistent with those found for the quenching systems with a nearly diffusion-controlled rate in liquid solution.[13−17] The values of α^{ex} and the bimolecular rate constant, $k^{S,bim,0}$ at 0.1 MPa, defined by

$$k^{S,bim,0} = k^S\left(\frac{k_{diff}}{k_{-diff}}\right)_0 = (k_{ic}^S + k_{et}^S)\left(\frac{k_{diff}}{k_{-diff}}\right)_0 \tag{15}$$

were determined from the least-squares slope and intercept, respectively, and are summarized in Table 5.

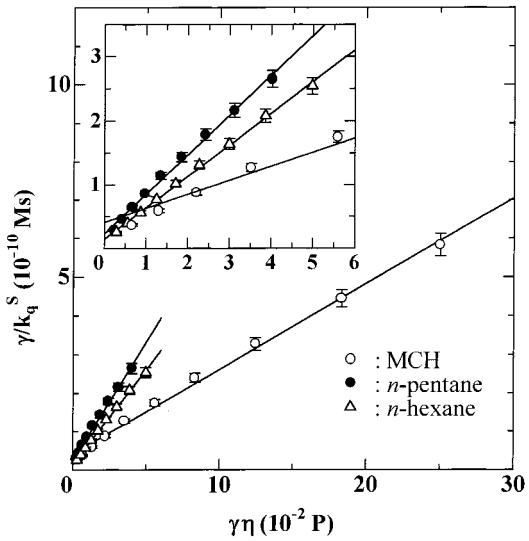

Figure 7. Plots of γ/k_q^S against $\gamma\eta$ in three solvents.

TABLE 5: Values of α^{ex} and α^{SW}(trunc) and Rate Parameters Associated with the Oxygen Quenching of Pyrene in Three Solvents

	α^{ex}	α^{SW} (trunc)	$k^{S,bim,0}/10^{10}$ M^{-1} s^{-1}	$k_{et}^{T,bim,0}/10^{10}$ M^{-1} s^{-1}	$k_{ic}^{T,bim,0}/10^{10}$ M^{-1} s^{-1}
n-pentane	1230 ± 40	1224	4.3 ± 0.7	1.4 ± 0.1	0.11 ± 0.01
n-hexane	980 ± 20	1182	6.9 ± 1.2	1.7 ± 0.1	0.13 ± 0.01
MCH	440 ± 20^a	1174	2.4 ± 0.4^b	1.2 ± 0.3	0.30 ± 0.08

[a] $\alpha^{ex} = 626 \pm 20$. [b] $k^{S,bim,0} = (5.95 \pm 0.64) \times 10^{10}$ M^{-1} s^{-1} at the pressure range from 0.1 to 150 MPa.

It has been shown that the value of α^{ex} is close to that, α^{SW}(trunc), evaluated by the semiempirical equation of Spernol and Wirts.[13−17] The values of α^{SW}(trunc) evaluated are shown in Table 5.[56] The value of α^{ex} is approximately equal to α^{SW}(trunc) in *n*-pentane and *n*-hexane, being consistent with those reported previously.[16] However, α^{ex} in MCH is significantly smaller compared to α^{SW}(trunc). By using our data reported previously,[34] the values of α^{ex} and α^{SW}(trunc) for the fluorescence quenching of 9,10-dimethylanthracene by oxygen in MCH were calculated to be 440 ± 20 and 1162, respectively; they are very close to the values of the present system. This indicates that α^{ex} is not predicted by α^{SW}(trunc) in MCH. The large difference between them implies that α^{ex} is related more significantly to the solvent properties including the molecular shape compared to *n*-pentane and *n*-hexane.

Contribution of Diffusion to the Fluorescence Quenching. Since the values of the bimolecular rate constant in the solvent cage at P MPa, $k^{S,bim}$, can be calculated by $k^{S,bim} = \gamma k^{S,bim,0}$, and those of k_{diff} reproduced by using α^{ex} and the solvent viscosity, η, according to eq 1, one can determine k_q^S(calc) by eq 16.[13,15−17]

$$k_q^{S}(\text{calc}) = \frac{k^{S,bim} k_{diff}}{k^{S,bim} + k_{diff}} \quad (16)$$

The pressure dependence of k_{diff}, $k^{S,bim}$, k_q^S(obs), and k_q^S(calc) thus determined is shown in Figure 8. It is noted in Figure 8 that $k^{S,bim}$ increases, whereas k_{diff} decreases monotonically with increasing pressure. Therefore, the difference between $k^{S,bim}$ and k_{diff} increases with increasing pressure. Thus, the competition of k_{diff} with $k^{S,bim}$ is significant at the lower pressure region, but the quenching approaches k_{diff} at the higher pressure region.

Pressure Dependence of the Quenching of the T_1 State and the Singlet Oxygen Yield. To investigate the quenching mechanism of the T_1 state, we plotted k_q^T/k_{diff} against k_{diff}, which is shown in Figure 9a. It is noted in Figure 9a that k_q^T/k_{diff} is smaller than 1/9 at high k_{diff}, that is, in the low-pressure region, and increases over 1/9 and approaches 4/9 as pressure increases further. According to Scheme 1, k_q^T/k_{diff} is expressed by

$$\frac{k_q^{T}}{k_{diff}} = \frac{1}{9}\frac{k_{et}^{T}}{k_{-diff} + k_{et}^{T}} + \frac{3}{9}\frac{k_{ic}^{T}}{k_{-diff} + k_{ic}^{T}} \quad (17)$$

In eq 17, when the quenching is fully diffusion-controlled, we have two limiting cases: (i) for the case of $k_{et}^T \gg k_{-diff}$ and $k_{ic}^T = 0$, $k_q^T/k_{diff} = 1/9$ and $f_\Delta^T = 1$; (ii) for the case k_{et}^T, $k_{ic}^T \gg k_{-diff}$, $k_q^T/k_{diff} = 4/9$ and $f_\Delta^T = 1/4$. When the quenching is reaction-controlled ($k_{-diff} \gg k_{et}^T$, k_{ic}^T), $k_q^T/k_{diff} = (k_{et}^T + 3k_{ic}^T)/9k_{-diff}$ and $f_\Delta^T = k_{et}^T/(k_{et}^T + 3k_{ic}^T)$. From the results of the pressure dependence of k_q^T/k_{diff} (Figure 9a), together with those obtained in this work that f_Δ^T in MCH decreases monotonically from 0.9 to 0.3 on going from 0.1 to 400 MPa, the quenching of T_1 state is not fully diffusion-controlled at the lower pressure region and approaches fully diffusion-controlled processes as pressure increases further. Furthermore, it is evident that the participation of the step of k_{ic}^T (Scheme 1) increases with increasing pressure, being in sharp contrast with the oxygen quenching of the T_1 state of 9-acetylanthracene for which the step of k_{is}^T is closed at high pressures up to 400 MPa.[34]

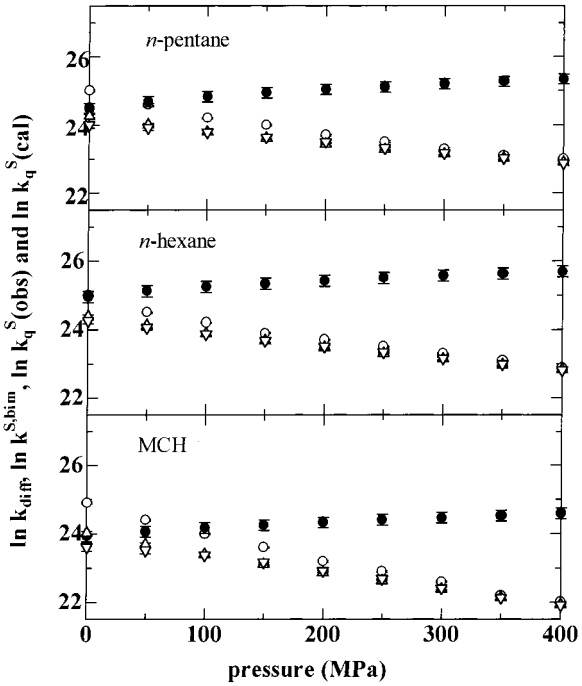

Figure 8. Pressure dependence of k_{diff} (○), $k^{S,bim}$ (●), k_q^S(obs) (△), and k_q^S(calc) (▽) for quenching by oxygen of the S_1 state of pyrene in three solvents.

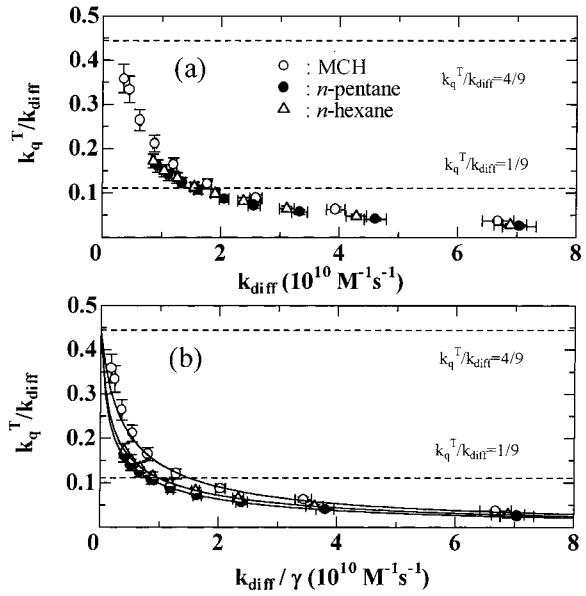

Figure 9. Plots of k_q^T/k_{diff} against (a) k_{diff} and (b) k_{diff}/γ in three solvents. The solid lines shown in (b) were drawn by the iterative nonlinear least-squares curve-fitting according to eq 18. The values of $k_{et}^{T,bim,0}$ and $k_{ic}^{T,bim,0}$ recovered are listed in Table 5 (see text).

From eq 17, we may obtain eq 18 by introducing the bimolecular quenching rate constant for the T_1 state at 0.1 MPa, $k_i^{T,bim,0}$ (i = et or ic) (see eq 15).

$$\frac{k_q^{T}}{k_{diff}} = \frac{1}{9}\frac{k_{et}^{T,bim,0}}{(k_{diff}/\gamma) + k_{et}^{T,bim,0}} + \frac{3}{9}\frac{k_{ic}^{T,bim,0}}{(k_{diff}/\gamma) + k_{ic}^{T,bim,0}} \quad (18)$$

The plots of k_q^T/k^{diff} against k_{diff}/γ are shown in Figure 9b. By assuming that $k_{et}^{T,bim,0}$ and $k_{ic}^{T,bim,0}$ are independent of pressure by the analogy with $k^{S,bim,0}$, we can evaluate these two parameters by curve fitting to eq 18 according to the nonlinear least-squares method. The best fit curves calculated are shown by the solid lines in Figure 8b, and the values of $k_{et}^{T,bim,0}$ and $k_{ic}^{T,bim,0}$ recovered are listed in Table 5. It can be seen in Figure 8b that the fitting is good in *n*-pentane and *n*-hexane, whereas it deviates slightly at the high-pressure region (>300 MPa) in MCH. The latter evidence in MCH implies that the enhanced viscosity induced by pressure causes participation of the intersystem crossing between the encounter complex pairs, as observed previously for the oxygen quenching of the T_1 state of 9-acetylanthracene[34] and the triplet−triplet annihilation of 2-acetonaphthone.[17]

Pressure Dependence of f_Δ^T and f_Δ^S. From eqs 9 and 18, one may derive eq 19.

$$f_\Delta^{T} = \left(\frac{k_{et}^{T,bim,0}}{(k_{diff}/\gamma) + k_{et}^{T,bim,0}}\right) \Bigg/ \left(\frac{k_{et}^{T,bim,0}}{(k_{diff}/\gamma) + k_{et}^{T,bim,0}} + \frac{3k_{ic}^{T,bim,0}}{(k_{diff}/\gamma) + k_{ic}^{T,bim,0}}\right) \quad (19)$$

The values of f_Δ^T at 0.1 MPa, calculated by using those of $k_{et}^{T,bim,0}$, $k_{ic}^{T,bim,0}$ (Table 5), and k_{diff}/γ, decrease moderately with increasing pressure; for example, they decrease from 0.60 ± 0.23, 0.78 ± 0.06, and 0.78 ± 0.05 to 0.32 ± 0.04, 0.54 ± 0.04, and 0.53 ± 0.02 in MCH, *n*-pentane, and *n*-hexane, respectively, when pressure increases from 0.1 to 400 MPa. The

values of f_Δ^T in MCH thus calculated agree qualitatively with those measured as a function of pressure in this work. The values 0.1 MPa are also in agreement with those in cylohexane (1.0)[28] and benzene (0.65).[29]

Finally, in the light of the present approach, f_Δ^S defined by eq 7 may be expressed by eq 20 using the bimolecular rate constants for the S_1 state at 0.1 MPa (see eq 15), $k_{ic}^{S,bim,0}$ and $k_{et}^{S,bim,0}$.

$$f_\Delta^S = \frac{k_{et}^{S,bim}}{k_{ic}^{S,bim} + k_{et}^{S,bim}} = \frac{k_{et}^{S,bim,0}}{k^{S,bim,0}} \qquad (20)$$

Thus, f_Δ^S should be independent of pressure. This is because singlet encounter complex pair alone in the quenching of the S_1 state is involved in the quenching (see Scheme 3). The overall quantum yield of singlet oxygen, Φ_Δ, in air-saturated solvent and its pressure dependence, which can be calculated by using f_Δ^S, f_Δ^T, and the parameters involved in eqs 6 and 8 according to eq 10, together with the reasonable assumption that $k_{et}^{S,bim,0}$ is approximately equal to $k_{et}^{T,bim,0}$, agrees qualitatively with the results shown in Figure 5 although the errors are large (the maximum error is ca. 40%).

Summary

It has been shown that the quenching by oxygen of the S_1 state in nonpolar solvents examined in this work is not fully but nearly diffusion-controlled. The contribution of diffusion was analyzed from the pressure-induced viscosity dependence of the quenching rate constant of the S_1 state, k_q^S, which was separated into the rate constants for diffusion, k_{diff}, and for bimolecular quenching in the solvent cage. It was found for the quenching of the T_1 state that the ratio of the quenching rate constant of the T_1 state k_q^T to k_{diff}, k_q^T/k_{diff}, decreases over 1/9 and approaches 4/9 with increasing pressure in the solvents examined. The results of the oxygen concentration dependence of the quantum yield for the formation of singlet oxygen, Φ_Δ, in MCH, together with those of the quantum yield for T_1 state at pressures up to 400 MPa, revealed that the branching ratio for the singlet oxygen formation in the T_1 state, f_Δ^T, decreases with increasing pressure. On the basis of Scheme 1, which involves the encounter complex pairs with singlet, triplet, and quintet spin multiplicities, the pressure dependence of k_q^T/k_{diff} and f_Δ^T was satisfactorily interpreted by eqs 18 and 19, respectively.

References and Notes

(1) Birks, J. B. *Photophysics of Aromatic Molecules*; Wiley-Interscience: New York, 1970; p 518.
(2) Saltiel, J.; Atwater, B. W. *Advances in Photochemistry*; Wiley-Interscience: New York, 1987; Vol. 14, p 1.
(3) Ware, W. R. *J. Phys. Chem.* **1962**, *66*, 455.
(4) Rice, S. A. In *Comrehensive Chemical Kinetics. Diffusion-Limited Reactions*; Bamford, C. H., Tripper, C. F. H., Compton, R. G., Eds.; Elsevier: Amsterdam, 1985; Vol. 25.
(5) Birks, J. B. *Organic Molecular Photophysics*; Wiley: New York, 1973; p 403.
(6) Evans, D. F.; Tominaga, T.; Chan, C. *J. Solution Chem.* **1979**, *8*, 461.
(7) Evans, D. F.; Tominaga, T.; Davis, H. T. *J. Chem. Phys.* **1981**, *74*, 1298.
(8) Spernol, A.; Wirtz, K. *Z. Naturforsch., A* **1953**, *8A*, 522.
(9) Gierer; A.; Wirtz, K. *Z. Naturforsch., A* **1953**, *8A*, 532.
(10) Schuh, H.-H.; Fischer, H. *Helv. Chim. Acta* **1978**, *61*, 2130.
(11) Saltiel, J.; Shannon, P. T.; Zafiriou, O. C.; Uriarte, K. *J. Am. Chem. Soc.* **1980**, *102*, 6799.
(12) Okamoto, M. *J. Phys. Chem. A* **1998**, *102*, 4751.
(13) Okamoto, M. *J. Phys. Chem. A* **2000**, *104*, 5029.
(14) Okamoto, M. *J. Phys. Chem. A* **2000**, *104*, 7518.
(15) Okamoto, M.; Wada, O. *J. Photochem. Photobiol., A: Chem*. **2001**, *138*, 87.
(16) Okamoto, M.; Wada, O.; Tanaka, F.; Hirayama, S. *J. Phys. Chem. A* **2001**, *105*, 566.
(17) Okamoto, M.; Teratsuji, T.; Tazuke, Y.; Hirayama, S. *J. Phys. Chem. A* **2001**, *105*, 4574.
(18) Yasuda, H.; Scully, A. D.; Hirayama, S.; Okamoto, M.; Tanaka, F. *J. Am. Chem. Soc.* **1990**, *112*, 6847.
(19) Hirayama, S.; Yasuda, H.; Scully, A. D.; Okamoto, M. *J. Phys. Chem.* **1994**, *98*, 4609.
(20) Gijzeman, O. L. J.; Kaufman, F.; Porter, G. *J. Chem. Soc., Faraday Trans. 2* **1973**, *69*, 708.
(21) Wilkinson, F.; McGravey, D. J.; Olea, A. F. *J. Am. Chem. Soc.* **1993**, *115*, 12151.
(22) Olea, A. F.; Wilkinson, F. *J. Phys. Chem.* **1995**, *99*, 4518.
(23) Redmond, R. W.; Braslavsky, S. E. *Chem. Phys. Lett.* **1988**, *148*, 523.
(24) Darmanyan, A. P.; Foote, C. S. *J. Phys. Chem.* **1993**, *97*, 5032.
(25) McGravey, D. J.; Szekeres, P. G.; Wilkinson, F. *Chem. Phys. Lett.* **1992**, *199*, 314.
(26) Wilkinson, F.; McGravey, D. J.; Olea, A. F. *J. Phys. Chem.* **1994**, *98*, 3762.
(27) Wilkinson, F.; Abdel-Shafi, A. A. *J. Phys. Chem. A* **1997**, *101*, 5509.
(28) Usui, Y.; Shimizu, N.; Mori, S. *Bull. Chem. Soc. Jpn.* **1992**, *65*, 897.
(29) McLean, A. J.; McGravey, D. J.; George Truscott, T.; Lambert, C. R.; Land, E. J. *J. Chem. Soc., Faraday Trans.* **1990**, *86*, 3075.
(30) Abdel-Shafi, A. A.; Wilkinson, F. *J. Phys. Chem. A* **2000**, *104*, 5747.
(31) Darmanyan, A. P.; Foote, C. S. *J. Phys. Chem.* **1992**, *96*, 3728.
(32) Garner, A.; Wilkinson, F. *Chem. Phys. Lett.* **1977**, *45*, 432.
(33) Grewer, C.; Brauer, H.-D. *J. Phys. Chem.* **1994**, *98*, 4230.
(34) Okamoto, M.; Tanaka, F.; Hirayama, S. *J. Phys. Chem.* **1998**, *102*, 10703.
(35) Tanaka, F.; Furuta, T.; Okamoto, M.; Hirayama, S. *Chem. Lett.* **2000**, 768.
(36) Kristiansen, M.; Scurlock, R. D.; Iu, K.-K.; Ogilby, P. R. *J. Phys. Chem.* **1991**, *95*, 5190.
(37) Scurlock, R. D.; Ogilby, P. R. *J. Photochem. Photobiol., A: Chem*. **1993**, *72*, 1.
(38) Okamoto, M.; Teranishi, H. *J. Phys. Chem.* **1984**, *88*, 5644.
(39) Okamoto, M.; Teranishi, H. *J. Am. Chem. Soc*. **1986**, *108*, 6378.
(40) Okamoto, M.; Sasaki, M. *J. Phys. Chem.* **1991**, *95*, 6548.
(41) Murrov, S. L. *Handbook of Photochemistry*; Marcel Dekker: New York, 1973.
(42) IUPAC Analytical Chemistry Division, Commission on Solubility Data. *Oxygen and Ozone*; Battino, R., Ed.; Solubility Data Series 7; Pergamon: Oxford, 1981.
(43) Bridgman, P. W. *Proc. Am. Acad. Arts Sci.* **1926**, *61*, 57.
(44) Brazier, D. W.; Freeman, G, R. *Can. J. Chem.* **1969**, *47*, 893.
(45) Oliveiria, C. M. B. P.; Wakeham, W. A. *Int. J. Thermophys*. **1992**, *13*, 773.
(46) Dymond, J. H.; Young, K. J.; Isdale, J. D. *Int. J. Thermophys*. **1980**, *1*, 345.
(47) Jonas, J.; Hasha, D.; Huang, S. G. *J. Chem. Phys.* **1979**, *71*, 15.
(48) Okamoto, M.; Tanaka, F. *J. Phys. Chem*. **1993**, *97*, 177.
(49) Okamoto, M.; Tanaka, F. *Phys. Chem. Chem. Phys*. **2000**, *2*, 5571.
(50) Okamoto, M.; Tanaka, F.; Teranishi, H. *J. Phys. Chem.* **1990**, *94*, 669.
(51) Schmidt, R.; Sekel, K.; Brauer, H.-D *Ber. Bunsen-Ges. Phys. Chem.* **1990**, *94*, 1100.
(52) In previous papers,[13−16] the quenching was assumed to involve the exciplex as well as the encounter complex formed between fluorophore, $^1M^*$, and quencher, Q. In this work, the contribution of the former is neglected since no evidence of the exciplex formation between the S_1 state of pyrene and O_2 in solution near room temperature has been observed.
(53) The radial distribution function at the closest approach distance, r_{M^*Q} ($=r_{M^*} + r_Q$) with the hard sphere assumption, $g(r_{M^*Q})$, is given by[54]

$$g(r_{M^*Q}) = \frac{1}{1-y} + \frac{3y}{(1-y)^2}\left(\frac{r_{red}}{r_S}\right) + \frac{2y^2}{(1-y)^3}\left(\frac{r_{red}}{r_S}\right)^2 \qquad (A\text{-}1)$$

where $r_{red} = r_{M^*} r_Q / r_{M^*Q}$ and y is the packing fraction, given in terms of the molar volume of solvent, V_S, by

$$y = \frac{4N_A \pi r_S^3}{3V_S} \qquad (A\text{-}2)$$

By using the values of r_S, r_{M^*}, and r_Q,[55] together with the data of the solvent density,[43−47] $g(r_{M^*Q})$ was calculated by eq A-1.

(54) Yoshimura, Y.; Nakahara, M. *J. Chem. Phys.* **1984**, *81*, 4080.
(55) Bondi, A. *J. Phys. Chem.* **1964**, *68*, 441.
(56) From the approximation by Spernorl and Wirtz, one may derive eq A-3.

$$k_{\mathrm{diff}} = \frac{2RTr_{\mathrm{M^*Q}}}{3000\eta}\left(\frac{1}{f_{\mathrm{M^*}}^{\mathrm{SW}} r_{\mathrm{M^*}}} + \frac{1}{f_{\mathrm{Q}}^{\mathrm{SW}} r_{\mathrm{Q}}}\right) \qquad \text{(A-3)}$$

where f_i^{SW} (i = M* or Q) represents a microfriction factor and is given by

$$f_i^{\mathrm{SW}} = (0.16 + 0.4r_i/r_{\mathrm{S}})(0.9 + 0.4T_{\mathrm{S}}^{\mathrm{r}} - 0.25T_i^{\mathrm{r}}) \qquad \text{(A-4)}$$

In eq A-4, T_s^{r} and T_i^{r} are the reduced temperatures of solvent and solute, respectively, which can be calculated by the method described elsewhere.[2,8,9] By comparing with eq 1, α^{SW} is given by

$$\alpha^{\mathrm{SW}} = \frac{1.2 \times 10^4}{r_{\mathrm{M^*Q}}}\left(\frac{1}{f_{\mathrm{M^*}}^{\mathrm{SW}} r_{\mathrm{M^*}}} + \frac{1}{f_{\mathrm{Q}}^{\mathrm{SW}} r_{\mathrm{Q}}}\right)^{-1} \qquad \text{(A-5)}$$

The values of α^{SW}(full) and α^{SW}(trunc) were evaluated by eq A-4 and by neglecting the second parenthetical quantity in eq A-4, respectively. The values of α^{SW}(trunc) are shown in Table 5 since α^{SW}(full) gives a negative value for the fluorophore/oxygen system.[15,16]